

Fast resonant target vibrating wire scanner for photon beam

S. G. Arutunian, M. Chung, G. S. Harutyunyan, A. V. Margaryan, E. G. Lazareva, L. M. Lazarev, and L. A. Shahinyan

Citation: [Review of Scientific Instruments](#) **87**, 023108 (2016); doi: 10.1063/1.4941837

View online: <http://dx.doi.org/10.1063/1.4941837>

View Table of Contents: <http://scitation.aip.org/content/aip/journal/rsi/87/2?ver=pdfcov>

Published by the [AIP Publishing](#)

Articles you may be interested in

[Beam Tail Measurements using Wire Scanners at DESY](#)

AIP Conf. Proc. **693**, 129 (2003); 10.1063/1.1638338

[Biasing Wire Scanners and Halo Scrapers for Measuring 6.7-MeV Proton-Beam Halo](#)

AIP Conf. Proc. **648**, 297 (2002); 10.1063/1.1524413

[Experiments with polarized photon beam at GRAAL](#)

AIP Conf. Proc. **570**, 198 (2001); 10.1063/1.1384065

[Slow wire scanner beam profile measurement for LEDA](#)

AIP Conf. Proc. **546**, 510 (2000); 10.1063/1.1342624

[APL Photonics](#)



SHIMADZU Excellence in Science **Powerful, Multi-functional UV-Vis-NIR and FTIR Spectrophotometers**

Providing the utmost in sensitivity, accuracy and resolution for applications in materials characterization and nano research

- Photovoltaics
- Polymers
- Thin films
- Paints
- Ceramics
- DNA film structures
- Coatings
- Packaging materials

[Click here to learn more](#)



Fast resonant target vibrating wire scanner for photon beam

S. G. Arutunian,^{1,a)} M. Chung,^{2,a)} G. S. Harutyunyan,¹ A. V. Margaryan,¹ E. G. Lazareva,¹
 L. M. Lazarev,¹ and L. A. Shahinyan¹

¹*Yerevan Physics Institute, Alikhanian Br. St. 2, Yerevan 0036, Armenia*

²*Ulsan National Institute of Science and Technology, Ulsan 689-798, South Korea*

(Received 22 September 2015; accepted 31 January 2016; published online 22 February 2016)

We propose a new type of wire scanner for beam profile measurements, based on the use of a vibrating wire as a scattering target. Synchronous measurements with the wire oscillation allow to detect only the signal coming from the scattering of the beam on the wire. This resonant method enables fast beam profiling in the presence of a high level of background. The developed wire scanner, called resonant target vibrating wire scanner, is applied to photon beam profiling, in which the photons reflected on the wire are measured by a fast photodiode. In addition, the proposed measurement principle is expected to monitor other types of beams as well, such as neutrons, protons, electrons, and ions. © 2016 AIP Publishing LLC. [<http://dx.doi.org/10.1063/1.4941837>]

I. INTRODUCTION

The operation principle of wire scanners, which are widely used for profile measurements of various types of beams, is based on the detection of secondary particles/radiation generated when the beam particles penetrate the wire. To pick out the beam signal from the high level of background, we consider using vibrating wire as a target whose oscillation frequency serves as a reference to separate noise and signal in the actual measurements. This idea was proposed in Refs. 1 and 2. In this paper, we realized this concept and developed a fast Resonant Target Vibrating Wire Scanner (RT-VWS) for photon beam profile measurements. The main idea of the method is to measure reflected signal coming from the scattering of the photon beam on the vibrating wire, synchronously with measuring the wire's oscillation frequency. Due to the high frequency of the wire oscillations (few kHz), it needs less than 1 ms of the measurement time at each scan position, which results in only tens of ms of total scan time. The differential signal is produced through two serial measurements of the photons reflected from the opposite positions of the vibrating wire oscillations. This procedure eliminates a high level of background noise falling on the photodiode during the photon measurements and also minimizes the noise in the measurement circuits. The proposed method is also applicable to scan beams of other types, e.g., neutrons (see Ref. 2), protons, electrons, and ions.

To apply the resonant target concept, we modified the vibrating wire monitors (VWMs) developed for low-flux beam profile measurements.^{3,4} These monitors are specially designed for beam halo measurements. Their operating principle is based on the precise detection of wire's temperature overheating. This overheating is caused by scattering of beam particles on the wire, so the measurement speed is necessarily slow to get a thermal balance during the position scan.

The oscillations of the wire are generated by the interaction of an AC drive current through the wire with a permanent magnetic field.⁵ A special feedback circuit selects the resonant frequency at which the AC current frequency is equal to the wire's natural frequency. The stabilization of mechanical oscillation process is provided by precise control of this current. Usually the peak-to-peak amplitude of the wire oscillation is a few times the wire diameter. It means that during the oscillation, the wire sweeps finite area in space and can be effectively treated as a moving target.

In Fig. 1(a), a nonuniform beam to be measured is presented by vertical lines with different thicknesses (the thicker, the higher beam intensity). The wire is vibrating with its first harmonic frequency and stretched perpendicular to the paper plane. The center of the wire is moving along the inclined segment which is indicated by a magenta arrow in Fig. 1(a) (not in the scale). The photons reflected on the vibrating wire are illustrated by horizontal lines whose thicknesses are proportional to the local beam flux. The photons are measured by fast photodiodes. To identify wire's maximal deviating position from the middle during the fast scan, we measure the signals synchronously with the wire's oscillation frequency. The required stroboscopic signal is provided by converting the sine-signal of autogenerator circuit into a rectangle-signal through a comparator circuit.

The measurement algorithm proposed in this work is based on subtraction of series of half-period measurements, which enables to eliminate background. Typically, the scan speed is much slower than the speed of the wire during the oscillation process so the following formula for profile gradient estimations can be used in case of negligible scan motion:

$$g_i = k_1 * \begin{cases} [S_{i+1} - S_i], & i = 1, 3, 5, \dots \\ -[S_{i+1} - S_i], & i = 2, 4, 6, \dots \end{cases}, \quad (1)$$

where S_i is the subsequent half-period photodiode measurement. The odd (even) i corresponds to the measurement at wire's left (right) position [see Fig. 1(b)]. Reversing the sign for odd and even estimations of g_i allows to take into account

^{a)}Authors to whom correspondence should be addressed. Electronic addresses: femto@yephi.am and mchung@unist.ac.kr.

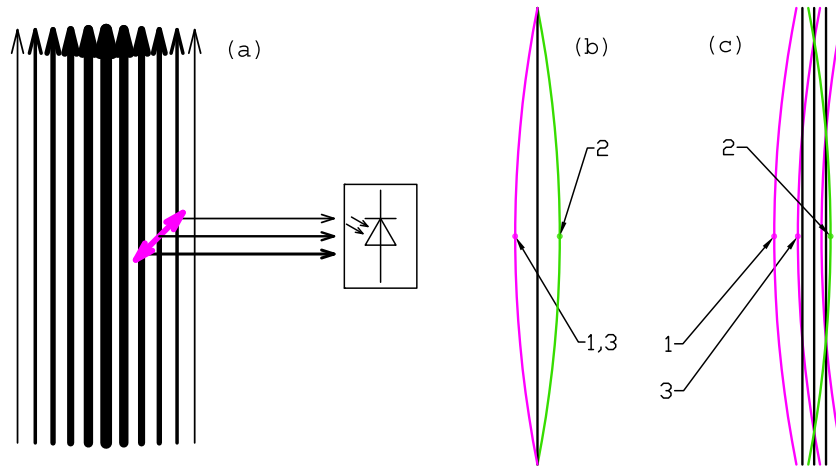


FIG. 1. Schematic view (a) of the measured beam with nonuniform profile. The nonuniform beam flux is represented by vertical lines with different thicknesses. The thicker lines correspond to the larger values of beam intensity. The direction of wire oscillation is perpendicular to the drawing plane, and the inclined segment (magenta line) indicates the movement of the vibrating wire center. The different fluxes of reflected photons at these positions, which are illustrated by horizontal arrows with different thicknesses, are measured by the fast photodiode. Schematic view (b) of the vibrating wire in the maximal deviating positions from the fixed stable position (black line): 1, 3—“left” measurements, 2—“right” measurements. Schematic view (c) of the vibrating wire moving to the right: during one period of the wire oscillation, the “left” measurements 1 and 3 shift proportional to scan speed. All schematics are not to scale.

only the spatial gradients and completely excludes the high-gradient temporal variations of the background. Formula (1) can be modified when the monitor is moving as a whole with a small scan speed [see Fig. 1(c)],

$$g_i = k_2 * \begin{cases} [S_{i+1} - S_i]/[a + V\tau/2], & i = 1, 3, 5, \dots \\ -[S_{i+1} - S_i]/[a - V\tau/2], & i = 2, 4, 6, \dots \end{cases} \quad (2)$$

where a is the wire oscillation amplitude, V is the scan speed, and τ is the wire oscillation period (assumed that $a/\tau \geq V$). Coefficients k_1 and k_2 connect the photodiode measurements to the absolute photon fluxes.

The total number of measurements during the scan of beam with size A will be

$$N = 2FA/V, \quad (3)$$

where $F = 1/\tau$ is the wire oscillation frequency.

To estimate the maximal scan speed, we imagine that at minimum 100 measurements should be made. In this case, we find

$$V_{MAX} = FA/50 \quad (4)$$

and minimal time of scan

$$t_S = 50/F \quad (5)$$

does not depend on the beam size.

In Table I, typical values for the parameters defined above are presented for two versions of the vibrating wire monitor.

TABLE I. Typical values for two different designs of the RT-VWS. Here, L —is the wire length, $2a/F$ —wire oscillation mean speed. The wire diameter in both cases is 0.1 mm.

L (mm)	F (Hz)	a (mm)	$2a/F$ (mm/s)	A (mm)	V_{MAX} (mm/s)	t_S (ms)	N
40	2500	0.15	750	3	150	20	100
80	1250	0.30	750	3	75	40	100

We note that the scan speed of the shorter wire can be increased twice. The scan speed is doubled with the shorter wire because the natural oscillation frequency of the shorter wire is doubled (with the assumption that the mechanical amplitudes of the oscillations remain approximately the same).

II. VWM

As a resonant target, we used the vibrating wire of the VWM with the following parameters: length of wire (L)—80 mm, monitor aperture (A)—27 mm, wire material—stainless steel, wire diameter—0.1 mm, and permanent magnets—samarium-cobalt. The schematic drawing of the VWM used in this experiment is presented in Fig. 2.

The wire oscillations are generated by a self-developed electronic auto-generation circuit (named StrinGen V4.0) with adjustable resistors in the feedback circuit. Magnetic poles are placed in such a way to generate the first harmonic wire oscillation. The typical value of the magnetic field strength in the gap is 0.7-0.8 T. The VWM can operate in the vacuum or in the air. In the vacuum, the frequency stability of the signal is less than 0.01 Hz. When the VWM is operating in the air, because of the convection, fluctuation in the frequency becomes larger (about 0.1 Hz). Nevertheless, the short-term frequency stability is good enough for use of the VWM wire as a resonant target in the air too. The impact of this fluctuation is quite negligible since the typical frequency measurement values are about 1-2 kHz. Typical oscillograms of the vibrating wire signals are presented in Fig. 3(a) (channel 2: signal directly from the wire, channel 1: amplified signal). The signal of channel 2 is in range of 20 mV and contains a lot of high frequency jitter originated from electromagnetic interference. The capacitances in the amplification unit filter this jitter out and transform the signal in the range of a few volts (signal of channel 1).

For the photodiode measurements synchronized with the wire oscillations, the amplified signal is sharpened by a comparator and used as a stroboscopic signal for the

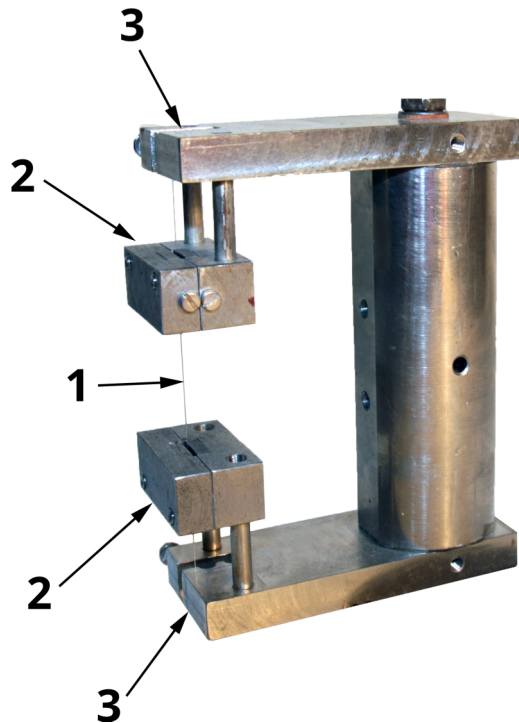


FIG. 2. Photograph of the VWM used in this experiment: 1—vibrating wire, 2—magnet system, and 3—wire supporting fork.

photodiode [see Fig. 3(b)]. As a triggering signal, the rising and falling edges of the stroboscopic signal are used with some time delays. The delays are adjusted experimentally to enable scattering measurements in the maximum deviation positions of the wire during oscillation process.

III. EXPERIMENT DESCRIPTION

A. Layout and preliminary experiments

To scan the laser beam profile by the RT-VWS, we design and construct a simple pendulum system. The VWM mounted on the bar pendulum allows to feed the monitor exactly in one

plane and eliminates all other types of swinging (e.g., rotation of VWM along the pendulum).

The length of the pendulum is 890 mm (from rotation axis to the wire center), and the initial amplitude of the pendulum oscillations is tunable and limited by a screw. Because of the friction in the rotation axis, the pendulum oscillations are damped, normally after 14-16 oscillations during one measurement cycle. The experiment layout and photo of the RT-VWS, laser, and photodiode are presented in Fig. 4.

The position and angle of the laser beam and photodiode are adjustable. In the present case [Fig. 4(b)], angles of the laser and photodiode plane with respect to the RT-VWS oscillation plane are set to be symmetrical. For the photodiode, we used a high speed and high sensitive silicone PIN VBPW34S photodiode (radiant sensitive area is 7.5 mm^2 , range of spectral bandwidth is 430-1100 nm, and rise/fall times are 100 ns).

For the laser, we used a red semiconductor laser (LED Lenser V9, wavelength 650 nm) with continuous pulse. The beam diameter is about 3 mm at the distance of 14 mm (vibrating wire position) and practically the same at the distance of 1 m. The power of the laser is less than 1 mW, so the luminous flux on the vibrating wire is about 14 mW/cm^2 and the spatial gradient of the luminous flux is $47 \text{ (mW/cm}^2\text{)/cm}$. When the vibrating wire is placed at the center of the laser beam spot, the corresponding overheating of the wire measured experimentally through the frequency shift of the monitor is about 4 mK. Of course, other types of the laser (e.g., pulsed or continuous He-Ne laser etc.) can also be used. The only restriction is that the wire overheating should not exceed few hundreds degrees Celsius and the spectral range of the photodiode should match to the laser wavelength.

Amplified signal from the photodiode is passed onto 13 bit ADC (MCP3301). Measurement duration at the ADC is set by a microcontroller (PIC18F252). To increase the transfer rate of the measurements to the personal computer (PC) and to make the measurements available online, the 115200 Baud rate has been chosen for the RS232 interface.

Before the scan of the laser beam, the photodiode measurement setup was tested in different conditions of the

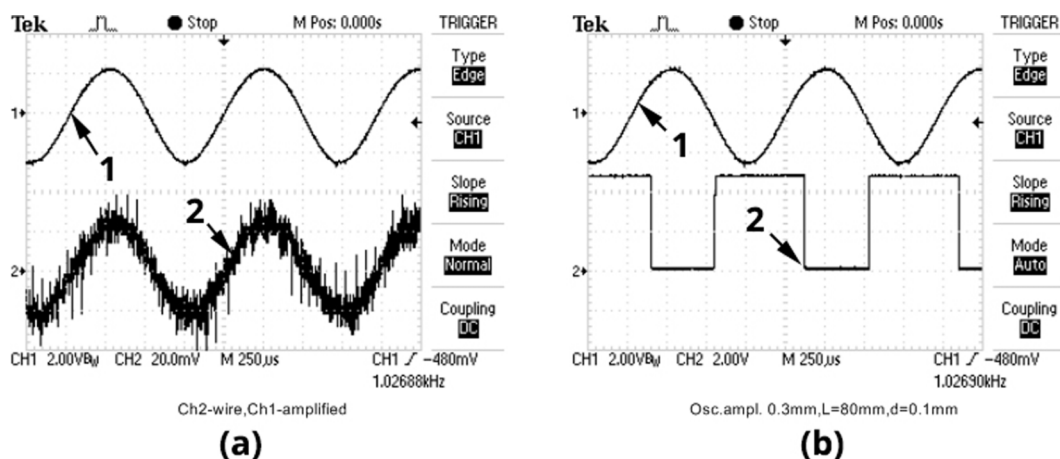


FIG. 3. (a) Oscillograms of vibrating wire signals: channel 2—signal with about 10 mV amplitude measured directly from the wire, channel 1—amplified signal. (b) Stroboscopic signal (bottom square wave) generated from the amplified current through the wire (upper sine curve). The signal in (b) is passed through a delay circuit and then it is transformed into a square signal by a pulse shaper. The arrows indicate the channel numbers.

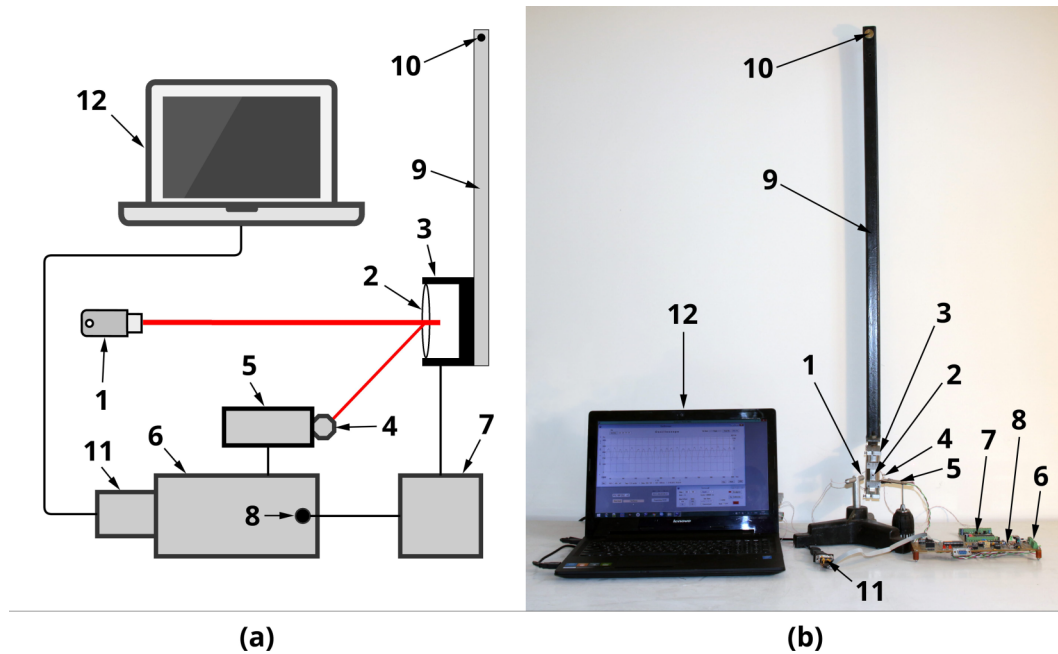


FIG. 4. Schematic block diagram (a) and photograph of experimental setup (b) 1—laser, 2—vibrating wire, 3—monitor, 4—photodiode, 5—photodiode front-end circuit, 6—photodiode measurement circuit, 7—wire oscillation autogenerator circuit, 8—stroboscopic input on the photodiode measurement circuit, 9—pendulum on which the monitor is mounted, 10—the axis of pendulum, 11—RS232 interface, and 12—PC.

ambient lightening. The main conclusion of these measurements was that the background of the laser beam measurements contains 50 Hz component mainly due to the ambient electric light. However, the 50 Hz component in the signal persists even without any electric light. We suspect that it is caused by electrical disturbances in the measurement circuit [see inset in Fig. 6(a)].

In order to find the phases of the maximal deviations of the wire from the stable position during the oscillation, the sweep of the photodiode signal was performed by changing the time delay from the rising/falling edges of the stroboscopic signal. In these measurements, the vibrating wire was located on the laser beam spot where the gradient of the laser beam profile is high enough. The photodiode signal over the oscillations period (about 1000 μs) is plotted in Fig. 5 as a function of the time delay from the rising edge. By analyzing this figure, one can see that the maximum signal, which corresponds to the signal from the leftmost position of the wire [positions 1 and 3 in Fig. 1(b)], is obtained at $delay_1 = 170 \mu\text{s}$. The

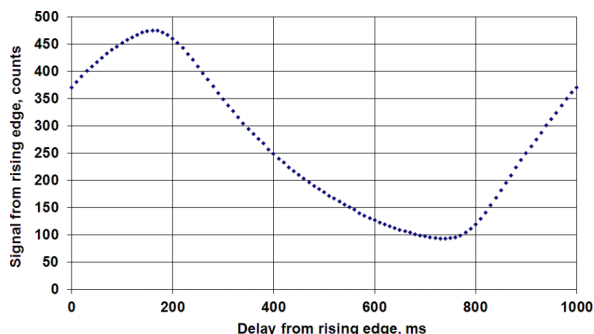


FIG. 5. Scan of the photodiode signals according to the time delay from the rising edge of stroboscopic signal. The vibrating wire is placed in a fixed position of the laser beam spot with a finite intensity gradient.

rightmost position of the wire corresponds to the time delay of 740 μs . Considering the pulse width in the stroboscopic signal [see Fig. 3(b)] was 580 μs , this time delay corresponds to $delay_2 = 160 \mu\text{s}$ from the falling edge. This signal sweep indeed defines the profile of the beam in a fixed position of the vibrating wire. So such measurements can provide information on the profiles of the ultrathin beams (when the beam sizes are about the amplitudes of the vibrating wire oscillations). More details on this subject will be discussed in the Conclusion.

To compare the measurements using the stroboscopic signal generated from the vibrating wire with those using an external signal generator, the following experiments were performed. The wire was placed under the laser beam in a fixed position with a finite flux gradient. The natural frequency of the vibrating wire was 1047.6 Hz.

In Fig. 6(a), photodiode measurements were initiated by the external generator with frequency approximately equal to the vibrating wire frequency (the frequency difference is less than 0.2 Hz). In this case, the serial measurements by the photodiode are separated by time interval approximately equal to the half-period of the vibrating wire oscillations. This time interval, however, does not exactly match to the maximal deviating position of the wire from the central position during the mechanical oscillation. As a result, we observed typical beating patterns, where the differential signal (the difference between two main signals) changes its sign with the periodicity of about few seconds [bottom magenta line in Fig. 6(a)]. The structure of the main signal from the photodiode contains high levels of 50 Hz components. However, such a structure is eliminated in the differential signal [see inset in Fig. 6(a)]. In case of measurements synchronized by the vibrating wire itself, both the main measurement and differential signals remain stable [see Fig. 6(b)]. By comparing Figs. 6(a) and 6(b), one can note that the local patterns (i.e., high levels

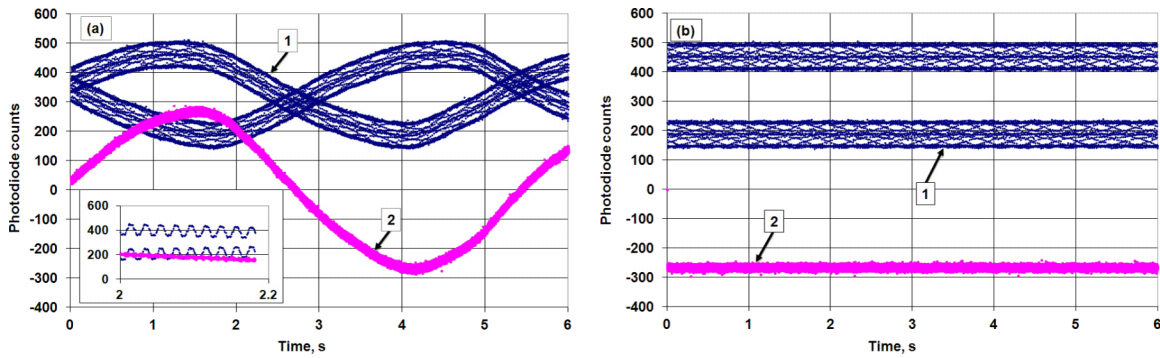


FIG. 6. Main (1, blue curves) and differential (2, magenta curves) signals of the laser beam reflections on the vibrating wire in cases when the measurements were synchronized by external generator (a) and by the vibrating wire itself (b).

of 50 Hz components) formed in the main signals are quite similar for both the measurements synchronized by external generator and by the vibrating wire itself.

B. Typical scan of laser beam profile

The scan of the laser beam profile was performed by swinging pendulum (see Fig. 7).

In the final damped position of the pendulum, the wire is parked away from the laser beam. For one pendulum oscillation period, two scans of the laser beam were made by the vibrating wire (the first scan from left to right, and the second from right to left).

The main measurement results during the pendulum oscillation process are presented in Fig. 8 (7 full oscillations of the pendulum and 14 full scans of the laser beam). The sine-like broad curve (upper dark blue in Fig. 8) presents the measurements of the photons originated from the reflections of the laser beam by the various parts of the RT-VWS (not from the vibrating wire). Reflections from the vibrating wire are seen as characteristic sparkles with different widths caused

by slowdown of the pendulum process. As one can see from Fig. 8 (bottom magenta curve), the differential signal obtained by the procedure described above is precisely picking up the events generated only when the vibrating wire crosses the laser beam.

Because of slowing-down of the pendulum oscillation motion, the temporal widths' of the vibrating wire scans are increased during the oscillation damping (the shortest at the first scan of the beam has 70 ms duration).

To illustrate the temporal dependence of the measurements and the corresponding differential signals, the fourteen scans in Fig. 8 are collected together in Figs. 9 and 10 [left to right directions (i.e., odd scans) in Fig. 9 and right to left directions (i.e., even scans) in Fig. 10].

For the recovery of the laser beam profile, we should integrate the differential signal along the spatial coordinate. By the analysis of the differential signal graph, we can detect the moments when the vibrating wire enters into and exits from the laser beam. These timestamps can serve as reference points for spatial coordinate recovering.

Assuming that the motion of the wire inside the laser beam is uniform, we can recover a laser beam profile. For 14th scan, we obtain the beam profile shown in Fig. 11(a).

It is obvious from Fig. 11(a) that we should take into account the fact that the real motion of the wire inside the beam has acceleration. To include this effect in the coordinate $x(t)$ of the vibrating wire, we approximate $x(t)$ by the following

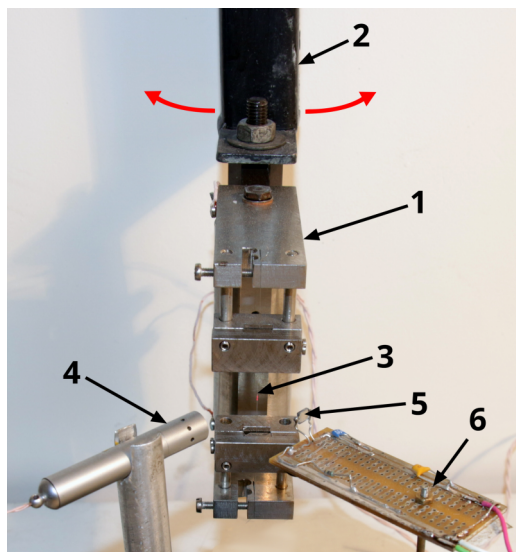


FIG. 7. Main view of RT-VWS (1) mounted on a pendulum (2), (3)—wire, (4)—laser, (5)—photodiode, and (6)—photodiode circuit. The swinging motion of the pendulum with RT-VWS is presented by arrows. The laser and photodiode remain fixed.

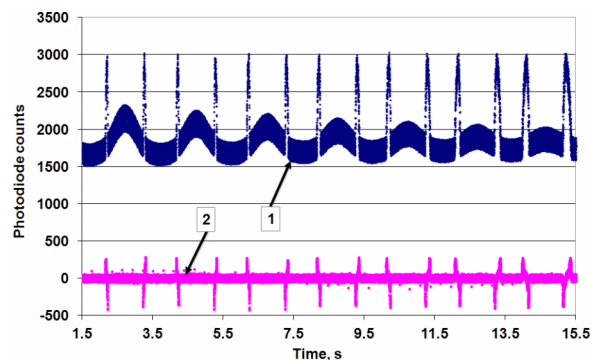


FIG. 8. Measurements of photodiode single (1, upper broad curve in dark blue), and corresponding differential signal (2, bottom curve in magenta) obtained by a series of scans with RT-VWS during one set of experiment (in the range of 1.5-15.5 s).

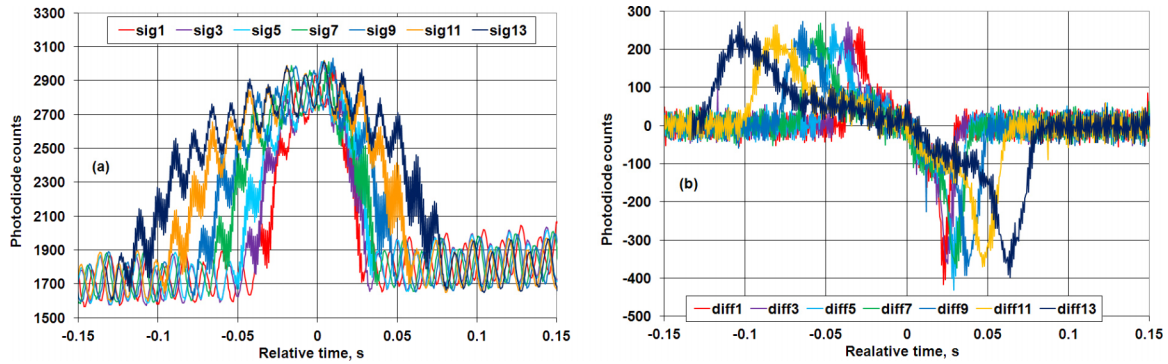


FIG. 9. The main (a) and differential signals (b) for odd scans (from left to right).

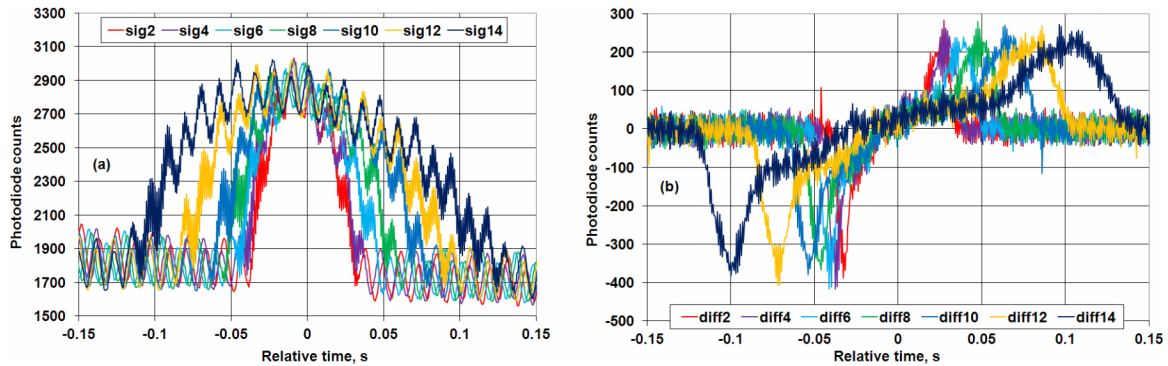


FIG. 10. The main (a) and differential signals (b) for even scans (from right to left).

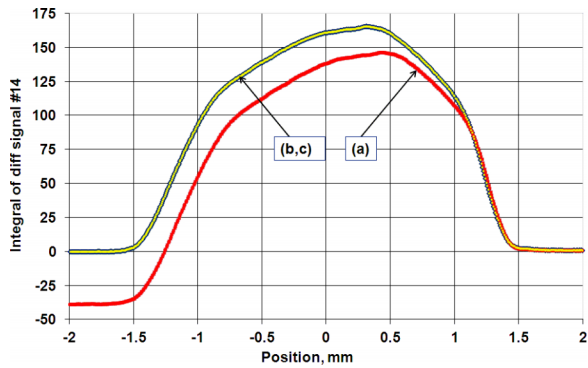


FIG. 11. Reconstruction of the laser beam profile by 14th scan using uniform motion approximation ((a), red line) and including corrections taking into account the accelerated motion ((b), dark blue wide line). Practically, the higher-order terms in the acceleration do not affect the final result ((c), yellow narrow line).

function:

$$x(t) = (A/2 - (A + c(t_2 - t_1)^2)(t - t_1)/(t_2 - t_1) + c(t - t_1)^2) \tag{6}$$

which provides necessary boundary conditions: $x(t_1) = A/2$ ($t_1 = 15.109$ s is entering time) and $x(t_2) = -A/2$ ($t_2 = 15.360$ s is exiting time). For the 14th scan, we consider that the scan is made from right to left. Here, A is the beam size defined in Eq. (3). The parameter c takes into account the accelerated motion and is found by a fitting procedure, which eliminates the offset in the tail levels. For the profile scan shown in Fig. 11, it results in $c = 8.3$ mm/s². The corrected profile according to Eq. (6) is shown in Fig. 11(b).

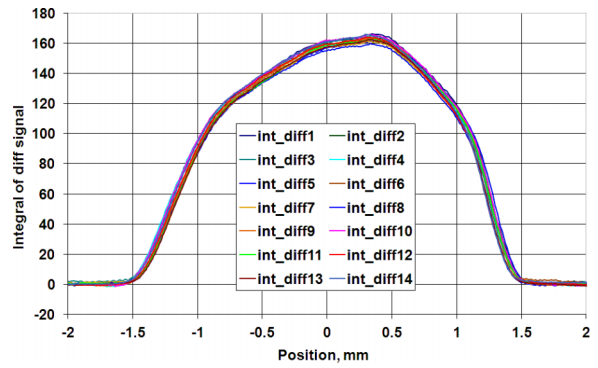


FIG. 12. Reconstruction of the laser beam profile using all 14 scans by applying uniform acceleration approximation.

After applying the same correction procedures to all scans, we reconstructed the laser beam profiles as presented in Fig. 12.

C. Resonant extraction of vibrating wire scattering

In this subsection, we present the result of laser beam scan in a special arrangement of laser and photodiode positions, in which the photodiode registers two very similar peaks with different origins—one is caused by reflections from the vibrating wire and the other from the holder of the monitor. The laser and photodiode are placed at an angle about 45° and at approximately the same distance of 14 mm, with respect to the pendulum’s swinging plane. In Fig. 13(a), the left peak corresponds to the signal of reflections from the vibrating

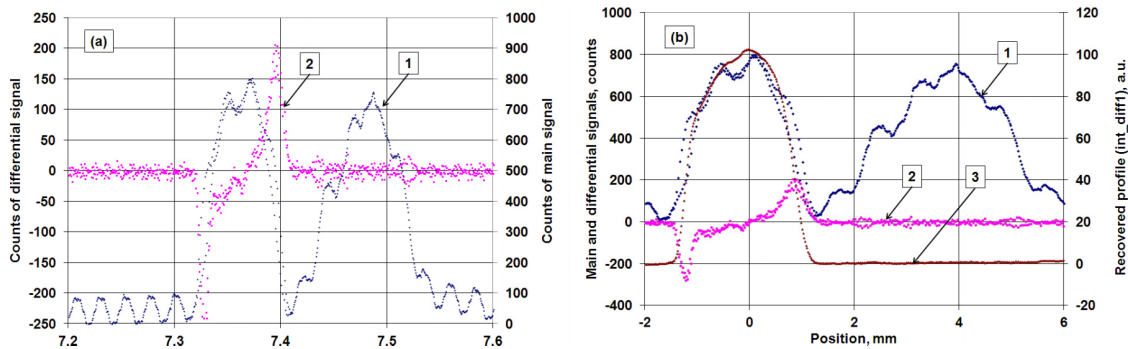


FIG. 13. (a) The photodiode measures reflections from both the vibrating wire and other mechanical parts of the RT-VWS (1, blue curve). Only the first type of the photodiode signal contributes to the differential signal (2, magenta curve). (b) The algorithm developed in this study recovers the laser beam profile (3, brown curve).

wire, and the right peak to the reflections from the RT-VWS's mechanical parts.

As one can see from Fig. 13(a), the differential signal only picks up the first peak (reflections on the vibrating wire) and completely filters out the second peak (reflections on the mechanical part), which allows us to easily recover the laser beam profile [Fig. 13(b)].

One can see the characteristic alternating signs in the differential signals [at 7.44 s and 7.52 s in Fig. 13(a), and at 2.2 mm and 5.1 mm in Fig. 13(b)] which are caused by high temporal gradients of the photon flux falling on the photodiode. However, according to our measurement algorithm [note two opposite signs in Eq. (1)], areas of opposite signs cancel out with each other in the integral which eventually yields the laser beam profile [Fig. 13(b)].

IV. CONCLUSION

The main advantage of the proposed resonant target vibrating wire scanner is the significant decrease in the scan time compared with the previous models of the VWM, in which the beam profile signal was obtained from the precise measurements of the vibrating frequency shift caused by changes in the equilibrium temperature. For example, 10 mA 10 keV proton beam with a size of about 2 mm overheats the stationary vibrating wire up to about 2200 K,⁹ which does not allow to use the previous type of the vibrating wire monitors. On the other hand, for the RT-VWM with a scan time of about 50 ms, the overheating of the tungsten wire over the room temperature is estimated to reach only 37 °C in the first order approximation. In this case, the object of the measurement should be secondary particles/photons generated as a result of the proton beam scattering. To prevent the damage of the photodiode, it should be possible to use phosphor sheets or scintillator strips. A fast scintillator with photomultiplier can also be used. Therefore, we expect the RT-VWS can be used even in this high radiation situation. Decrease of the scan time will also be helpful for use of rotating array of the vibrating wires for tomography.¹⁰

In the new type of the scanner presented in this paper, a differential principle of the measurements has been applied. The new method can effectively remove all types of unwanted backgrounds from the main signal generated during beam particles/radiation scattering on the vibrating wire. Due to this

procedure, much simpler detectors can be used for measuring beam scattering. The method is applicable for different types of the beam by simply choosing a proper detector for each case. For photon beams, fast photodiodes can be used, for charged particles, scintillators with photomultipliers (see, e.g., Ref. 6), and for neutrons, wires covered by gadolinium layer,² etc. We note that for particle beam profiling, special types of photodiodes (such as diamond-based detectors) can be also used.⁷ The idea of detecting visible light emitted when a high current beam heats a vibrating wire (see, e.g., Ref. 8) can be investigated as well.

It is interesting to note that the two principles (slow measurement of the vibrating wire frequency shift caused by overheating, and fast measurement of the differential signal of the beam scattering on the vibrating wire) can be combined into one unit with different scales of scan speed: slow at halo area and fast in the beam core. As mentioned in Sec. III A, the resonant target method can be applied for a VWM in a fixed position as a scanner of ultrathin beam. In this case, the measurements should be done by sweeping time delay from the stroboscopic signal generated by the vibrating wire (see, for example, Fig. 5). This method can be useful for thin X-rays (30-100 μm sizes¹¹), low energy electron beams for various applications,¹² synchrotron radiation,¹³ and small-size accelerator beam diagnostics for high energy machines.^{14,15}

ACKNOWLEDGMENTS

Authors would like to thank S. L. Egiazaryan for the help in the assembly of the experimental components and express special thanks to G. M. Davtyan for great support. This work was partly supported by the National Research Foundation of Korea (NRF) grant funded by the Korean government (MSIP: Ministry of Science, ICT and Future Planning) (No. NRF-2015M2B2A4033273).

¹S. G. Arutunian and A. V. Margaryan, "Oscillating wire as a 'Resonant Target' for beam," in *Proceedings of International Particle Accelerator Conference IPAC2014, Dresden, Germany* (Joint Accelerator Conferences Website (JACoW), 2014), pp. 3412–3414, ISBN: 978-3-95450-132-8.

²S. G. Arutunian, J. Bergoz, M. Chung, G. S. Harutyunyan, and E. G. Lazareva, "Thermal neutron flux monitors based on vibrating wire," *Nucl. Instrum. Methods Phys. Res., Sect. A* **797**, 37–43 (2015).

- ³S. G. Arutunian, "Vibrating wire sensors for beam instrumentation," in *Beam Instrumentation Workshop, BIW08, Lake Tahoe, USA, 4-8 May* (Joint Accelerator Conferences Website (JACoW), 2008), pp. 1–7.
- ⁴S. G. Arutunian, M. Werner, and K. Wittenburg, "Beam tail measurements by wire scanners at DESY," in *ICFA Advanced Beam Dynamic Workshop: Beam Halo Dynamics, Diagnostics, and Collimation (HALO'03) (in Conjunction with 3rd Workshop on Beam-Beam Interaction)* (Gurney's Inn, Montauk, NY, USA, 2003), 19-23 May.
- ⁵S. G. Arutunian, A. E. Avetisyan, M. M. Davtyan, G. S. Harutyunyan, I. E. Vasiniuk, M. Chung, and V. Scarpine, "Large aperture vibrating wire monitor with two mechanically coupled wires for beam halo measurements," *Phys. Rev. Spec. Top.—Accel. Beams* **17**, 032802 (2014).
- ⁶T. Moore, N. I. Agladze, I. V. Bazarov, A. Bartnik, J. Dobbins, B. Dunham, S. Full, Y. Li, X. Liu, J. Savino, and K. Smolenski, "Fast wire scanner for intense electron beams," *Phys. Rev. Spec. Top.—Accel. Beams* **17**, 022801 (2014).
- ⁷H. Aoyagi, Y. Asano, T. Itoga, N. Nariyama, T. Bizen, T. Tanaka, and H. Kitamura, "Pulse-mode measurement of electron beam halo using diamond-based detector," *Phys. Rev. Spec. Top.—Accel. Beams* **15**, 022801 (2012).
- ⁸S. Johansson, P.-O. Eriksson, J. Rajander, J.-O. Lill, and O. Solin, "Wire scanner for beam profile of high current particle accelerator beams," in *The 14-th International Workshop on Targetry and Target Chemistry WTTTC14, Playa del Carmen, Mexico, 26-29 August 2012* (AIP Conference Proceedings, 2012), p. 20.
- ⁹M. A. Aginian, S. G. Arutunian, A. V. Margaryan *et al.*, "Vibrating wire monitor evaluation, an application to calculate resolution and dynamic range," *Journal of Contemporary Physics* (Armenian Academy of Sciences) (to be published).
- ¹⁰J. Alonso and S. G. Arutunian, "Complex beam profile reconstruction, a novel rotating array of vibrating wires," in *Proceedings of International Particle Accelerator Conference IPAC2014, Dresden, Germany* (Joint Accelerator Conferences Website (JACoW), 2014), pp. 3415–3417, ISBN: 978-3-95450-132-8.
- ¹¹A. G. Touryanskii and I. V. Pirshin, "A method for the formation of ultrathin X-ray beams," *Instrum. Exp. Tech.* **43**(5), 664–670 (2000).
- ¹²A. V. Scherbakov, A. L. Goncharov, V. K. Dragunov, and A. O. Gladyshev, "Development of an electron-beam welding unit for small-size pieces," *Russ. Electr. Eng.* **84**(6), 318–323 (2013).
- ¹³T. Mitsuhashi, "Measurement of small transverse beam size using interferometry," in *Proceedings of DIPAC2001* (Joint Accelerator Conferences Website (JACoW), 2001), pp. 26–30.
- ¹⁴A. S. Hernandez, N. Milas, M. Rohrer, V. Schlott, A. Streun, A. Andersson, and J. Breunlin, "The new SLS beam size monitor, first results," in *IPAC2013* (Joint Accelerator Conferences Website (JACoW), 2013), pp. 759–761, ISBN: 978-3-95450-122-9.
- ¹⁵R. Chehab, "A small survey on beam diagnostics for small size beam," <http://www-linac.kek.jp/seminar/chehab-lecturenote-transparencies/BeamDiagnostics.pdf>, 2002.